CONTINUOUS METRICS AND MESH OPTIMIZATION

Francois Courty [a], David Leservoisier [b], Paul-Louis George [c], Alain Dervieux [a]

[a] *INRIA, BP 93, 06902 Sophia Antipolis, France*

[b] *SNECMA-Villaroche, 77550 Moissy-Cramayel, France*

[c] *INRIA, BP 105, 78153 Le Chesnais, France*

Abstract

This paper describes a functional analysis modelisation of the problem of the optimal mesh for representing at best in L^p a twice continuous differentiable function defined on the plane. It relies on an abstract mesh model, the "continous metrics" allowing a variational analysis and the identification of an optimum. Anisotropic optimal meshes can then be specified. We present a few numerical illustrations related to numerical solution representation and image compression.

Key words: mesh, adaptation, approximation, interpolation, compression, metrics

1 Introduction

Something is rotten in the state of CFD approximation: CFD researchers have spent decades to build "second-order accurate schemes" and when they apply them to industrial problems convergence is not at the expected second order. When they address theorists about this problem, they receive the answer that their Navier-Stokes flow fields are smooth but they have steep gradients. And therefore it might happen that second order convergence, which is only an asymptotical property, will indeed apply, but only for extremely fine meshes that are not usable in practice.
In fact, in order to answer to the expectation of these practitioners, a new theory of approximation, taking into account mesh adaptation is being built. New theoretical developments are specifying progressively how meshes should be adapted in order to get an error lower than a prescribed threshold. The

derivation of *a posteriori* errors is an important topic in this direction, see for example [1], [2],[10]. The numerical order of the convergence to the continuous is also very frequently evaluated from the variation of error with respect to the number of nodes (see for example [18]).

Also progressively, the mesh becomes a part of the unknowns in the system to solve.

In the case where the mesh is seeked among a set of deformations of a reference one, many works in the literature proposed the mesh deformation or equivalently mesh coordinates as the solution of a particular system coupled with the discrete Partial Differential Equation (PDE) under study. See for example [5],[16]. In that case the mesh topology is prescribed by the user and may be not adequate to the adaptation.
Conversely, in the case where the user does not wish to fix the topology, but instead, wants the algorithm to find it, then the definition of a system the solution of which is the adapted mesh is much more difficult. Firstly, two meshes can have very different topologies and give about the same accuracy. Secondly, it is difficult to investigate in a general set of meshes the connectivities of which are generally described by integers, booleans,...

This kind of remarks have motivated some researchers to represent meshes by continuous functions. They can be for example the (scalar) local mesh size over the computational domain. From the local mesh size, it is possible to derive a majorant for the local truncation error. But this majorant does not give a perfect idea of the local error because local stretching effects are not taken into account.

In many recent publications, see for example [3],[4], [12], and [13], the local stretching is also modelled thanks to the definition of a **metric** non-scalar field computed from the discrete PDE solution.
Then an error equidistribution argument is used for specifying a new mesh from the metric and then re-solve the PDE.

The main purpose of the present work is to explore several outputs of an analysis in which we keep everything *undiscretized.*

In the first step presented in this paper, we focus on the easier problem of adapting a mesh to the best ($\mathcal{P}_1$) interpolation of a given analytic function. The problem of the best adapted metric can be cast into an abstract optimization problem and the optimal metric can be exhibited. The mathematical model also allows to reproduce some convergence-to-the limit behaviors, giving some prediction of the discrete case properties.

We shall first consider the 1D case and recall how a continuous metric is defined, how the interpolation error can be modelled, and how a calculus of variation produces an optimal metric. The 1D case allows for a large overview of many possible extensions.
Then we shall propose a model for the 2D case. The error model will be derived from an accurate error estimate. Then again we propose a definition of the best metric. This time, mesh anisotropy is taken into account.
We complete these theoretical statements by a series of numerical experiments in order to show examples for which behavior predicted by the theory are indeed observed. We illustrate how the "best interpolation" problem that we address can be related to compression issues and thus, validating the proposed method in a rather different field of applications.

2 Continuous metric in an interval

In the one-dimensional case, a mesh is uniquely specified by a metric. After some definitions concerning the metric, we recall an estimate of the interpolation error and then show how an optimal metric can be derived.

2.1 Definitions

2.1.0.1 A metric on a given set allows to define the distance between two arbitrary element of it. We shall call metric on interval $[a, b]$ a (strictly) positive continuous function $\mathcal{M} : x \to \mathcal{M}(x)$ defined on $[a, b]$. It specifies, for any c and d of this interval the length of segment cd as follows:

$$L_{\mathcal{M}}(cd) = \int_c^d \sqrt{\mathcal{M}}(s) \quad ds \tag{1}$$

Let us consider a mesh of interval $[a, b]$ with N nodes. It is a subdivision $x_0 = a \ < \ x_1, ..., x_i \ < \ x_{i+1}, ..., x_{N-1} \ < \ x_N = b$ of this interval.

A consequence of the above definition is that a metric can prescribe a particular class of meshes. Indeed, we shall say that a mesh conforms to metric $\mathcal{M}$ if and only if the following relation, unitary element length holds:
for any element $[x_i, x_{i+1}]$, *we have* $\int_{x_i}^{x_{i+1}} \sqrt{\mathcal{M}} dx = 1$.

If we introduce the local continuous mesh size $m_{\mathcal{M}} = \mathcal{M}^{-1/2}$ we have:

for any element $[x_i, x_{i+1}]$, $\int_{x_i}^{x_{i+1}} \frac{1}{m_{\mathcal{M}}}\, dx = 1$,
which shows that when $m_{\mathcal{M}}$ is a constant function, it is nothing other than the element size.
Another way to understand this is to introduce the local continuous node density $d = 1/m$:

for any interval $[x_i, x_{i+1}]$, *we have* $\int_{x_i}^{x_{i+1}} d\ dx = 1$.
It can be verified that the number of nodes (or equivalently intervals) of the mesh is specified by the metric. It is given by:

$$C(\mathcal{M}) = \int_a^b \sqrt{\mathcal{M}} dx = \int_a^b 1/m dx = \int_a^b d\ dx. \tag{2}$$

If $C(\mathcal{M})$ is a positive integer, only one mesh is decribed by it, if $C(\mathcal{M})$ is not an integer, no mesh is described by it.

2.2 Interpolation error

2.2.0.2 We propose now to modelize the error related to a given metric. Since the metric determines the local mesh size, it also determines the interpolation error resulting of the application of an interpolator on the mesh. We modelize now this error as a continous function of the metric.

Let us consider :

- A uniform mesh, i.e.: $x_0 < x_1 < ... < x_N$ with $x_i = x_0 + \frac{i}{N-1}(x_N - x_0)$,
- A function u, regular enough, defined on a segment $[a, b]$, $a = x_i, b = x_{i+1}$,
- h is not necessarily small,
- $\Pi_h u$ the $\mathcal{P}_1$ interpolation of u on every interval $[a, b]$ of the mesh.
- Assuming $\Pi_h u(a) = u(a)$ and $\Pi_h u(b) = u(b)$, the approximation error is defined by:

$$e = u - \Pi_h u. \tag{3}$$

2.2.0.3 For any x in $[a, b]$, there exists t_1 in $[0, 1]$ such that :

$$\begin{aligned} e(a) &= (u - \Pi_h u)(a) \qquad (4)\\ &= (u - \Pi_h u)(x) + (a - x)(u - \Pi_h u)'(x) + \frac{(a-x)^2}{2} u''(x + t_1(a - x)). \end{aligned}$$

Let us denote $e = (u - \Pi_h u)$, for x between a and b, there exists a way such that t_2 in $[0, 1]$:

$$
\begin{aligned}
e(b) &= (u - \Pi_h u)(b) && (5) \\
&= (u - \Pi_h u)(x) + (b - x)(u - \Pi_h u)'(x) + \frac{(b - x)^2}{2} u''(x + t_2(b - x)).
\end{aligned}
$$

Finding a majorant of $e = (u - \Pi_h u)$ leads to look for a point x such that :

$$
e'(x) = (u - \Pi_h u)'(x) = 0. \tag{6}
$$

Using (5) and (6), while $e(a) = e(b) = 0$, we have for this x :

$$
0 = (u - \Pi_h u)(x) + \frac{(a - x)^2}{2} u''(x + t_1(a - x)), \tag{7}
$$

$$
0 = (u - \Pi_h u)(x) + \frac{(b - x)^2}{2} u''(x + t_2(b - x)). \tag{8}
$$

Here, t_1 and t_2 depend on x. By addition we get:

$$
\begin{aligned}
0 = {} & 2(u - \Pi_h u)(x) + \frac{(a - x)^2}{2} u''(x + t_1(a - x)) \\
& + \frac{(b - x)^2}{2} u''(x + t_2(b - x)).
\end{aligned} \tag{9}
$$

Thus :

$$
\begin{aligned}
2(u - \Pi_h u)(x) = {} & -\frac{(a - x)^2}{2} u''(x + t_1(a - x)) \\
& - \frac{(b - x)^2}{2} u''(x + t_2(b - x)),
\end{aligned} \tag{10}
$$

and

$$
|(u - \Pi_h u)(x)| \leq \frac{1}{2}(|\frac{(a - x)^2}{2}| + |\frac{(b - x)^2}{2}|)M, \tag{11}
$$

where M is a majorant of $|u''|$ over $[a, b]$. Then :

$$
|(u - \Pi_h u)(x)| \leq \frac{1}{2}(\frac{(a - x)^2}{2} + \frac{(b - x)^2}{2})M. \tag{12}
$$

Taking the maximum, we have:

$$|(u - \Pi_h u)(x)| \leq \frac{1}{2} \max_{\xi \in I}(\frac{(a-\xi)^2}{2} + \frac{(b-\xi)^2}{2}))M. \tag{13}$$

The maximum is reached for $\xi_0 = \frac{(a+b)}{2}$, this implies, $\forall \xi \in I$:

$$|e(\xi)| = |(u - \Pi_h u)(\xi)| \leq \frac{(b-a)^2}{8} M. \tag{14}$$

This estimate, after it has been modelled in terms of continuous functions, will contribute to the continuous problem statement.

2.3 Optimal metric

2.3.1 Optimality condition for norm L^α

2.3.1.1 We can now *modelize* the error resulting from using a $\mathcal{P}_1$ interpolation on a mesh respecting a given metric $\mathcal{M}$. The analysis of previous section suggests (neglecting higher-order terms) to take the following model:

$$|e_{\mathcal{M}}(x)| = (d_{\mathcal{M}}(x))^{-2} |u''(x)|. \tag{15}$$

where $d_{\mathcal{M}}(x)$ is the node density of the mesh, or equivalently the inverse local mesh size, i.e. the inverse of $m_{\mathcal{M}}(x)$. We want now to find the minimum with respect to metric $\mathcal{M}$ of the L^α $(0 < \alpha < \infty)$ norm of the error $e_{\mathcal{M}}$:

$$\min_{\mathcal{M}} \ (|e_{\mathcal{M}}(x)|)^\alpha_{L^\alpha} = \min_{\mathcal{M} \in K} \ \frac{1}{2} \int_a^b (d_{\mathcal{M}}(x)^{-2} |u''(x)|)^\alpha ds. \tag{16}$$

2.3.1.2 In order to get a non-trivial infinitely fine solution, the space of admissible metrics is chosen in order to prescribe the number of nodes:

$$C(M) = \bar{C}(d) = \int_a^b d(x) dx \ = N. \tag{17}$$

which gives a linear constraint.
In order to get (at least formally) optimality condition, we can derive the

functional of (16) with respect to d:

$$-2\alpha \int_a^b d^{-2\alpha-1} \left(|u''|\right)^\alpha \delta d \; ds \geq 0 \, , \, \forall \delta d : \int_a^b \delta d = 0. \tag{18}$$

Thus:

$$d_{opt}(x) = Cte.|u''(x)|^{\frac{\alpha}{2\alpha+1}} \tag{19}$$

and taking into account the constraint $\bar{C}(d) = N$, we get:

$$d_{opt}(x) = \frac{N}{\int |u''|^{\frac{\alpha}{2\alpha+1}} ds} \; |u''(x)|^{\frac{\alpha}{2\alpha+1}}, \tag{20}$$

or in terms of the local mesh size:

$$m_{opt}(x) = \frac{\int |u''|^{\frac{\alpha}{2\alpha+1}} ds}{N} \; |u''(x)|^{\frac{-\alpha}{2\alpha+1}}. \tag{21}$$

Remark 1 *For identifying the above formally optimal metric as a rigorous minimum of the initial problem, several questions remain open.*
Firstly, it is not clear whether there is a minimum. probably, it is not reasonable to seek it without any smoothness assumption, for example it seems useful to assume that the metric is bounded in a Sobolev space. This would correspond to an assumption on the smoothness of the underlying meshes: no element with vanishing measure, no sudden variation of elements shape and size.
Secondly, in the case we make an assumption leading to a sufficient compacity of admissible set, the question of uniqueness should be addressed.
Lastly, a local analysis is possible, the Hessian of the functional is positive, which shows that the formal optimum is at least a local optimum in any smooth enough subset of the set of constraints.

Remark 2 *The local mesh size, naturally inverse proportional to the number of nodes, is defined by (21) only if the second derivative u'' never vanishes. In practice, we replace $|u''|$ by $\max(\varepsilon, |u''|)$, with a small positive ε.*

The minimum of the functional writes:

$$(\mathcal{E}_\alpha^{opt})^\alpha \;=\; 1/2 \left(\frac{\int |u''|^{\frac{\alpha}{2\alpha+1}} ds}{N} \right)^{2\alpha} \int_a^b |u''(s)|^{\frac{\alpha}{2\alpha+1}} ds. \tag{22}$$

2.3.2 Examples

- For the case of L^1 norm: This is a rather classical norm in image processing,

$$m_{opt}(x) \;=\; \frac{\int |u''|^{1/3} ds}{N} \; |u''(x)|^{-1/3} \tag{23}$$

- For the case of the L^2 norm: This is the natural option for PDE's,

$$m_{opt}(x) \;=\; \frac{\int |u''|^{2/5} ds}{N} |u''(x)|^{-2/5} \; . \tag{24}$$

- For the case of L^∞ norm: We can make the exposant tend to infinity and *formally* get:

$$m_{opt}(x) \;=\; \frac{\int |u''|^{1/2} ds}{N} |u''(x)|^{-1/2} \; . \tag{25}$$

Remark 3: *In the last case, introducing d_{opt}:*

$$d_{opt}(x) = \frac{N}{\int |u''|^{\frac{1}{2}} ds} \; |u''(x)|^{\frac{1}{2}}. \tag{26}$$

in (15) gives a uniform error,

$$|e_{\mathcal{M}}(x)| = (d(x))^{-2} |u''(x)| = \frac{(\int |u''|^{\frac{1}{2}} ds)^2}{N^2}, \tag{27}$$

which is nothing else that the usual error repartition formula. We also remark that the optimal error magnitude is determined by the $\mathcal{L}^{1/2}$ norm of the second derivative.

If we take the α-th root of expression (22), we get:

$$\mathcal{E}_\alpha^{opt} \;=\; 1/2 \left(\frac{\int |u''|^{\frac{\alpha}{2\alpha+1}} ds}{N} \right)^2 \; (\int_0^1 |u''(s)|^{\frac{\alpha}{2\alpha+1}} ds)^{1/\alpha}, \tag{28}$$

and passing to the limit:

$$\mathcal{E}_\infty^{opt} \;=\; \frac{1}{N^2} \left(\int |u''|^{\frac{1}{2}} ds \right)^2 . \tag{29}$$

Remark 4: *The power $1/2$ of the second derivative $|u''|$ is related with the accuracy order of the interpolation. The same analysis can be done with a more* *accurate interpolation, that is typically with an error model of κ-th order:*

$$|e_{\mathcal{M}}(x)| \quad = \quad (d_{\mathcal{M}}(x))^{\kappa}|u^{(\kappa)}| \ ; \tag{30}$$

in that case the optimal power is $\frac{\alpha}{\kappa\alpha+1}$ and always smaller than $1/\kappa$.

2.4 Convergence order of the continuous metric model

Let us examine how to look for an optimal metric in the *discontinuous case*. When a $\mathcal{P}_1$ interpolation is choosen, we modelize the error as :

$$\int_0^1 |e_{\mathcal{M}}(x)|^{\alpha} ds = \int_0^1 (m^2|\delta^{-2}(u(x+\delta) - 2u(x) + u(x-\delta))|)^{\alpha} ds. \tag{31}$$

Where δ is smaller than m. We observe that the differential quotient:

$\delta^{-2}(u(x+\delta) - 2u(x) + u(x-\delta))$:

- is close to $\frac{\partial^2 u}{\partial x^2}$ where u is regular,

- or of the order of δ^{-2} at singularities of u.

Moreover, since u is bounded,

$$||\delta^{-2}(u(x+\delta) - 2u(x) + u(x-\delta))||_{L^{1/2}} \ \ \textit{is bounded independantly of} \ \ \delta. \tag{32}$$

The calculus of variations gives now:

$$m_N(x) = Cte.|(|\delta^{-2}(u(x+\delta) - 2u(x) + u(x-\delta))|(x))|^{\frac{-2}{5}}, \tag{33}$$

and the resulting optimal error in L^2 writes:

$$\text{Error} = \frac{2}{N^2} \ \left(\int |\delta^{-2}(u(x+\delta) - 2u(x) + u(x-\delta))|^{\frac{2}{5}}\right)^{\frac{5}{2}} < \frac{K}{N^2}$$

where K is a bounded constant, due to (32). We deduce that the adaptive strategy is formally of second-order accuracy.

3 The 2D case

3.0.0.1 We propose an extended model for the interpolation error and then apply again a variation calculus.

3.1 Definition

3.1.1 Main notations

Let u be a twice continuously differentiable function from a subset Ω of R^2 in R.
To any triangulation $\mathcal{T}_h$ of Ω corresponds an interpolation $\mathcal{P}^1$ of u that we denote by $\Pi_h u$.

For the local error analysis:

- We consider $K = [a, b, c]$, a triangle the diameter h_{max} of which does not tend to zero.
- We consider u, a function from R^2 to R that is $\mathcal{C}^2$,
- We denote by $\Pi_h u$, the linear interpolate of u over K,
- We assume that u and $\Pi_h u$ coincide in a, b and c.

We want to find a good majorant to the error $e = u - \Pi_h u$ on $K = [a, b, c]$.

3.1.2 Hessian matrix $\mathcal{H}$

3.1.2.1 The Taylor formula writes:

$$\begin{aligned} u(\vec{x} + \delta\vec{x}) = {} & u(\vec{x}) + \frac{\partial u}{\partial x}(\vec{x}).\delta\vec{x} \\ & + \frac{1}{2}\frac{\partial^2 u}{\partial x^2}(\vec{x}).\delta\vec{x}.\delta\vec{x} + \ldots \end{aligned} \tag{34}$$

with:

$$\delta\vec{x} = \begin{pmatrix} \delta x \\ \delta y \end{pmatrix} \tag{35}$$

$$\frac{\partial^2 u}{\partial x^2}(\vec{x}).\delta\vec{x}.\delta\vec{x} \Leftrightarrow \begin{bmatrix} a & b \\ b & c \end{bmatrix} * \begin{pmatrix} \alpha \\ \beta \end{pmatrix} . \begin{pmatrix} \gamma \\ \zeta \end{pmatrix} = (a.\alpha + b.\beta).\gamma + (b.\alpha + c.\beta).\zeta \tag{36}$$

The Hessian of u is denoted by:

$$\mathcal{H} = \begin{pmatrix} \frac{\partial^2 u}{\partial x^2} & \frac{\partial^2 u}{\partial x.\partial y} \\ \frac{\partial^2 u}{\partial x.\partial y} & \frac{\partial^2 u}{\partial y^2} \end{pmatrix} \tag{37}$$

$\mathcal{H}$ is diagonalizable and can be written:

$$\mathcal{H} = \mathcal{R} * \begin{pmatrix} \lambda_1 & 0 \\ 0 & \lambda_2 \end{pmatrix} * \mathcal{R}^{-1} \tag{38}$$

We introduce the rotation matrix $\mathcal{R}$ passing from the usual (x, y) coordinate system to a system (ξ, η):

$$\mathcal{H} \equiv \mathcal{R}\widehat{\mathcal{H}}\mathcal{R}^{-1}. \tag{39}$$

Which means that:

$$\lambda_1 = \frac{\partial^2 u}{\partial \xi^2} \tag{40}$$

and

$$\lambda_2 = \frac{\partial^2 u}{\partial \eta^2}. \tag{41}$$

3.2 Metric $\mathcal{M}$

3.2.0.2 The family of metrics we shall consider contains a tensor field depending on (x, y) and defined as follows from two rotations $\mathcal{S}$ and $\mathcal{S}^{-1}$:

$$\mathcal{M}(x, y) = \mathcal{S}^{-1} \begin{pmatrix} \frac{1}{m_\xi}^2 & 0 \\ 0 & \frac{1}{m_\eta}^2 \end{pmatrix} \mathcal{S}, \tag{42}$$

where $\mathcal{S}, m_\xi$, and m_η depend on x and y. The coefficients m_ξ, and m_η are the local mesh sizes in each of the two directions ξ and η defined by the rotation $\mathcal{R}$. Similarly to the 1D case, the length $L_{\vec{u}}$ of vector $\vec{u}$ in metric $\mathcal{M}$ is defined as follows:

$$L_{\vec{u}} = \int_0^1 \sqrt{\vec{u}.\mathcal{M}.\vec{u}} \;\; ds. \tag{43}$$

Quantities $\frac{1}{m_\xi}$ and $\frac{1}{m_\eta}$ represent the number of mesh elements by unit length following respectively axes ξ and η.

3.3 Complexity $C(\mathcal{M})$

3.3.0.3 In a similar way to the 1D case, we associate to a metric $\mathcal{M}$ the complexity or total number of nodes computed from an integral of mesh density, i.e. from ε, m_ξ and m_η, on an area of ε^2 area unit.

$$C(\mathcal{M}) = \int_\Omega \sqrt{\mathcal{M}} ds = \int_\Omega \frac{1}{m_\xi}\frac{1}{m_\eta}\, dxdy. \tag{44}$$

Let $d(\xi, \eta)$ be the local density of nodes for the metric $\mathcal{M}$. It is equal to $\frac{1}{m_\xi}.\frac{1}{m_\eta}$.

Lemma 3 *If a tensorial mesh with $N+1$ nodes in each direction satisfies ideally the metric $\mathcal{M}$ then :*

$$\int_0^1 m_\xi^{-1}.m_\eta^{-1}(s)\, ds = \sum_i \int_{x_i}^{x_{i+1}} \int_{y_i}^{y_{i+1}} d(s)\, ds = \sum_{i=1}^{N}\sum_{i=1}^{N}(1) = N^2. \tag{45}$$

3.4 Rough majoration

Let us write $(u - \Pi_h u)$ in the neighboring of a:

$$\begin{aligned}(u-\Pi_h u)(a) = &(u-\Pi_h u)(x) + < \vec{xa}, \nabla(u-\Pi_h u)(x) > \\ &+ \frac{1}{2} < \vec{ax}, H_u(x + t_1\vec{xa})\vec{ax} >,\end{aligned} \tag{46}$$

where t_1 is between 0 and 1 and depends on x and a(we denote by $< \vec{v}, H(.)\vec{v} >$ the scalar product related to $H(.)$). Similarly, for b and c, we get:

$$\begin{aligned}(u-\Pi_h u)(b) = &(u-\Pi_h u)(x) + < \vec{xb}, \nabla(u-\Pi_h u)(x) > \\ &+ \frac{1}{2} < \vec{bx}, H_u(x + t_2\vec{xb})\vec{bx} >,\end{aligned} \tag{47}$$

$$\begin{aligned}(u-\Pi_h u)(c) = &(u-\Pi_h u)(x) + < \vec{xc}, \nabla(u-\Pi_h u)(x) > \\ &+ \frac{1}{2} < \vec{cx}, H_u(x + t_3\vec{xc})\vec{cx} > .\end{aligned} \tag{48}$$

In order to have a majorant of $e = (u - \Pi_h u)$, we look for a point x where the extremum is attained. If x is in K then:

$$\nabla(u - \Pi_h u)(x) = 0, \tag{49}$$

or:

$$< v\vec{e}c, \nabla(u - \Pi_h u)(x) >= 0, \tag{50}$$

for any $v\vec{e}c$ in R^2 or in K.

Using the three above extension and remaking that $e(a) = e(b) = e(c) = 0$, we get:

$$\begin{aligned} 0 &= (u - \Pi_h u)(x) + \frac{1}{2} < \vec{ax}, H_u(x + t_1 \vec{xa})\vec{ax} >, \\ 0 &= (u - \Pi_h u)(x) + \frac{1}{2} < \vec{bx}, H_u(x + t_2 \vec{xb})\vec{bx} >, \\ 0 &= (u - \Pi_h u)(x) + \frac{1}{2} < \vec{cx}, H_u(x + t_3 \vec{xc})\vec{cx} > \end{aligned} \tag{51}$$

and by addition:

$$\begin{aligned} 0 = & 3(u - \Pi_h u)(x) \\ & + \frac{1}{2} < \vec{ax}, H_u(x + t_1 \vec{xa})\vec{ax} > \\ & + \frac{1}{2} < \vec{bx}, H_u(x + t_2 \vec{xb})\vec{bx} > \\ & + \frac{1}{2} < \vec{cx}, H_u(x + t_3 \vec{xc})\vec{cx} > . \end{aligned} \tag{52}$$

Let M be a real number such that:

$$M = \max_{x \in K} \left(\max_{v\vec{e}c \in R^2} \frac{|v\vec{e}c, H_u(x) v\vec{e}c|}{||v\vec{e}c||^2} \right), \tag{53}$$

Then:

$$|(u - \Pi_h u)(x)| \leq \frac{1}{6} \left(||\vec{ax}||^2 + ||\vec{bx}||^2 + ||\vec{cx}||^2 \right) M. \tag{54}$$

By definition,

$$x = \lambda_a a + \lambda_b b + \lambda_c c, \tag{55}$$

with:

$$\lambda_a + \lambda_b + \lambda_c = 1. \tag{56}$$

Thus:

$$\begin{aligned} \vec{ax} &= \lambda_b \vec{ab} + \lambda_c \vec{ac}, \\ \vec{bx} &= \lambda_c \vec{bc} + \lambda_a \vec{ba}, \\ \vec{cx} &= \lambda_a \vec{ca} + \lambda_b \vec{cb}. \end{aligned} \tag{57}$$

We deduce that:

$$\begin{aligned} ||\vec{ax}||^2 + ||\vec{bx}||^2 + ||\vec{cx}||^2 \leq\ & (\lambda_a^2 + \lambda_b^2)||\vec{ab}||^2 \\ & + (\lambda_a^2 + \lambda_c^2)||\vec{ac}||^2 \\ & + (\lambda_b^2 + \lambda_c^2)||\vec{bc}||^2 \\ & + 2(\lambda_a \lambda_b)| < \vec{ca}, \vec{cb} > | \\ & + 2(\lambda_a \lambda_c)| < \vec{ba}, \vec{bc} > | \\ & + 2(\lambda_b \lambda_c)| < \vec{ab}, \vec{ac} > |. \end{aligned} \tag{58}$$

If we denote by L the length of the largest edge, then:

$$||\vec{ax}||^2 + ||\vec{bx}||^2 + ||\vec{cx}||^2 \leq 2(\lambda_a^2 + \lambda_b^2 + \lambda_c^2 + \lambda_a\lambda_b + \lambda_a\lambda_c + \lambda_b\lambda_c)L^2. \tag{59}$$

One easily verifys that the extremum is reached at:

$$\lambda_a = \lambda_b = \lambda_c = \frac{1}{3} \tag{60}$$

and thus the majoration writes:

$$|(u - \Pi_h u)(x)| \leq \frac{2}{9} L^2 M. \tag{61}$$

This result suggests the form of the majoration to get in the case of an arbitrary dimension d:

$$\begin{aligned} |(u - \Pi_h u)(x)| &\leq \frac{1}{2}\frac{1}{1+d}\left(\frac{d(d+1)}{(d+1)^2} + 2\frac{d(d-1)}{2}\frac{d+1}{d+1}^2\right) L^2 M \\ &= \frac{1}{2}\left(\frac{d}{1+d}\right)^2 L^2 M. \end{aligned} \tag{62}$$

We return to the case where the extremum is not reached in K. Then it corresponds to an edge, let us say the edge ab. The gradient vanishes on ab and it follows that:

$$0 = 2(u - \Pi_h u)(x) + \frac{1}{2} < \vec{ax}, H_u(x + t_1 \vec{xa})\vec{ax} > \\ + \frac{1}{2} < \vec{bx}, H_u(x + t_2 \vec{xb})\vec{bx} > . \tag{63}$$

Let M such that:

$$M = \max_{x \in \vec{ab}} \left(\max_{v\vec{e}c \in ab} \frac{| < v\vec{e}c, H_u(x) v\vec{e}c > |}{||v\vec{e}c||^2} \right), \tag{64}$$

then:

$$|(u - \Pi_h u)(x)| \leq \frac{1}{4} \left(||\vec{ax}||^2 + ||\vec{bx}||^2 \right) M. \tag{65}$$

Since $x = \lambda_a a + \lambda_b b$, we recover the majoration established in one dimension:

$$|(u - \Pi_h u)(x)| \leq \frac{1}{8} \left(||\vec{ab}||^2 \right) M. \tag{66}$$

And the:

$$|(u - \Pi_h u)(x)| \leq \frac{1}{8} L^2 M. \tag{67}$$

This result is better than (61) but does not provide any information concerning the possible anisotropy of the function and therefore cannot be used in order to prescribe any stretching in the mesh.

3.5 An anisotropic majoration

Anisotropic majorations are the topic of many current researchers, see for example [9]. We present here a result adapted to our needs. Let us assume that the point x where the maximum is attained is closer to a than to b or c. We assume also that x is in K (not on an edge). We denote by a' the intersection point between ax and the edge facing a in K, i.e. bc. We develop e from a:

$$
\begin{aligned}
e(a) &= (u-\Pi_h u)(a) \\
&= (u-\Pi_h u)(x) + < \vec{xa}, \nabla(u-\Pi_h u)(x) > \\
&+ \int_0^1 (1-t) < \vec{xa}, H_u(x+t\vec{xa})\vec{ax} > dt.
\end{aligned} \tag{68}
$$

Since x is closer to a, the number λ, such that $\vec{ax} = \lambda \vec{aa'}$, is smaller than $\frac{2}{3}$:

$$
\begin{aligned}
|e(x)| &= |\int_0^1 (1-t)\lambda^2 < \vec{aa'}, H_u(a+t\vec{xa})\vec{aa'} > dt|, \\
|e(x)| &\leq \frac{4}{9}|\int_0^1 (1-t) < \vec{aa'}, H_u(a+t\vec{xa})\vec{aa'} > dt|, \\
|e(x)| &\leq \frac{4}{9}|\int_0^1 (1-t)dt| \max_{t\in[0,1]} | < \vec{aa'}, H_u(a+t\vec{xa})\vec{aa'} > |,
\end{aligned} \tag{69}
$$

Then:

$$
|e(x)| \leq \frac{2}{9}|\max_{y\in\vec{aa'}} |\vec{aa'}, H_u(y)\vec{aa'} > |, \tag{70}
$$

or:

$$
|e(x)| \leq \frac{2}{9}|\max_{y\in K} |\vec{aa'}, H_u(y)\vec{aa'} > |. \tag{71}
$$

The above recurrence formula then reappears with the following constant:

$$
\lambda^2|\int_0^1 (1-t)dt = \frac{1}{2}\left(\frac{d}{d+1}\right)^2. \tag{72}
$$

The case where x is located on an edge, let us say edge ab, will eventually lead to the same majoration:

$$
|e(x)| \leq \frac{1}{8}\max_{y\in ab} | < \vec{ab}, H_u(y)\vec{ab} > |, \tag{73}
$$

which can be formally written as above (with $a' = b$ and noting that $\frac{1}{8} < \frac{2}{9}$).

3.6.0.4 We consider first the optimal anisotropic metric. The local mesh size is defined as a unique scalar field, $m(x,y)$ or equivalently the node density by area unit $d(x,y) = 1/m^2(x,y)$. The total number of nodes is given by:

$$C(\mathcal{M}) = \int_\Omega d(x,y)\ dxdy. \tag{74}$$

For error modelling, we get inspiration from the above rough estimate:

$$e_{\mathcal{M}}(x,y) \ = m^2(x,y)M(x,y) \ = \ d^{-1}(x,y)M(x,y)\ . \tag{75}$$

where M, above defined is taken equal to the largest absolute value of eigenmodes of the Hessian of u.
Let us minimize the $\mathcal{L}^\alpha$ norm of this error under the constraint of a number of nodes equal to N:

$$\min_{\mathcal{M}} \ \frac{1}{2}\int_\Omega M^\alpha\ d^{-\alpha}\ dxdy \tag{76}$$

under the constraint $C(\mathcal{M}) = N$.

The optimality conditions are:

$$-\alpha\int_\Omega M^\alpha\ d^{-\alpha-1}\ \delta d\ dxdy\ \leq\ 0 \tag{77}$$

for any δd such that $\int_\Omega \delta d\ dxdy = 0$,

or taking into account the constraint:

$$d_{opt}(x) = \frac{N}{\int_\Omega M^{\frac{\alpha}{-\alpha-1}} dxdy}\ M(x,y)^{\frac{\alpha}{\alpha+1}}. \tag{78}$$

Remark 5: *Again the case $\alpha = +\infty$ gives $d = M$, that is the error isorepartition.*

In terms of the local mesh size m it gives:

$$m_{opt}(x) = \frac{(\int_\Omega M^{\frac{\alpha}{-\alpha-1}} ds)^{1/2}}{N}\ M(x,y)^{\frac{-\alpha}{2\alpha+2}}. \tag{79}$$

In particular for $\alpha = 2$, the exponent in (79) is $1/3$.

3.7 Minimization of the interpolation error (II)

3.7.0.5 Considering an anisotropic family of metrics, we return to the general notations of Sections 3.1, 3.2,and 3.3.

3.7.1 Optimization problem

3.7.1.1 We assume that function u has bounded second derivatives $\frac{\partial^2 u}{\partial x^2}, \frac{\partial^2 u}{\partial x \partial y}, \frac{\partial^2 u}{\partial y^2}$. We admit that the best metric should be choosen among metrics that are aligned with the Hessian of u. We then consider metrics $\mathcal{M}$:

$$\mathcal{M}_{x,y} = \mathcal{R}_{\mathcal{M}}^{-1} \begin{pmatrix} (m_\xi)^{-2} & 0 \\ 0 & (m_\eta)^{-2} \end{pmatrix} \mathcal{R}_{\mathcal{M}} \tag{80}$$

such that:

$$\mathcal{R}_{\mathcal{M}} \quad = \quad \mathcal{R}_u \ , \tag{81}$$

where $\mathcal{R}_u$ is the rotation which diagonalize the Hessian of u:

$$\mathcal{H}_u = \begin{pmatrix} \frac{\partial^2 u}{\partial x^2} & \frac{\partial^2 u}{\partial x.\partial y} \\ \frac{\partial^2 u}{\partial x.\partial y} & \frac{\partial^2 u}{\partial y^2} \end{pmatrix} = \mathcal{R} * \begin{pmatrix} \frac{\partial^2 u}{\partial \xi^2} & 0 \\ 0 & \frac{\partial^2 u}{\partial \eta^2} \end{pmatrix} * \mathcal{R}^{-1} \tag{82}$$

As above, for simplicity, the second derivatives $\frac{\partial^2 u}{\partial \xi^2}$ et $\frac{\partial^2 u}{\partial \eta^2}$ are assumed to be of absolute value strictly positive.
The previous error estimate lead to consider the following *anisotropic error continuous model*:

$$\mathcal{E}_\alpha = \int \left(|\frac{\partial^2 u}{\partial \xi^2}|.m_\xi^2 + |\frac{\partial^2 u}{\partial \eta^2}|.m_\eta^2 \right)^\alpha \ dxdy \ . \tag{83}$$

The optimal metric minimize the functional $\mathcal{E}_\alpha$ under the constraint $C(\mathcal{M}) = N^2$:

$$\min_{\mathcal{M}} \int \left(|\frac{\partial^2 u}{\partial \xi^2}|.m_\xi^2 + |\frac{\partial^2 u}{\partial \eta^2}|.m_\eta^2 \right)^\alpha \ dxdy \tag{84}$$

under the constraint $\int m_\xi{}^{-1} m_\eta{}^{-1}\ dxdy = N^2$.

The optimality system writes:

$$\begin{aligned}\mathcal{E}'_\alpha(\mathcal{M})\delta\mathcal{M} &= 0, \\ \forall \delta\mathcal{M}, \quad C'(\mathcal{M}_{opt}).\delta\mathcal{M} &= 0.\end{aligned} \tag{85}$$

The second equation can be used for writing a relation between $\mathcal{M}$ and $\mathcal{C}$:

$$\begin{aligned} C'(\mathcal{M}_{opt}).\delta\mathcal{M} &= 0, \\ &\Updownarrow \\ \int \frac{-1}{m_\xi}.\frac{\delta m_\eta}{m_\eta^2} + \frac{-1}{m_\eta}.\frac{\delta m_\xi}{m_\xi^2} &= 0, \\ &\Updownarrow \\ \int \frac{1}{m_\xi}.\delta m_\eta + \frac{1}{m_\eta}.\delta m_\xi &= 0. \end{aligned} \tag{86}$$

One can write:

$$\begin{pmatrix} \delta m_\xi \\ \delta m_\eta \end{pmatrix} = \zeta \begin{pmatrix} -m_\xi \\ m_\eta \end{pmatrix}. \tag{87}$$

Equation (85) will be verified for any couple $(\delta m_\xi, \delta m_\eta)$ such that (87) holds at least for one scalar function ζ of (x, y).

Let us develop equation (85) :

$$\int \left(|\frac{\partial^2 u}{\partial \xi^2}| m_\xi^2 + |\frac{\partial^2 u}{\partial \eta^2}|.m_\eta^2 \right)^{\alpha-1} \left(|\frac{\partial^2 u}{\partial \xi^2}| m_\xi \delta m_\xi + |\frac{\partial^2 u}{\partial \eta^2}| m_\eta \delta m_\eta \right) dxdy = 0.(88)$$

Due to statement (87) we can replace δm_ξ and δm_η :

$$\int \left(\left| |\frac{\partial^2 u}{\partial \xi^2}| m_\xi^2 + |\frac{\partial^2 u}{\partial \eta^2}|.m_\eta^2 \right|^{\alpha-1} \right) \zeta \left(-|\frac{\partial^2 u}{\partial \xi^2}| m_\xi m_\xi + |\frac{\partial^2 u}{\partial \eta^2}| m_\eta m_\eta \right) dxdy = 0\ .(89)$$

Since m_η, m_ξ and the second derivatives of u do not vanish, this will be zero for any function ζ if:

$$|\frac{\partial^2 u}{\partial \xi^2}|.m_\xi^2 = |\frac{\partial^2 u}{\partial \eta^2}|.m_\eta^2. \tag{90}$$

From which we can derive the ratio between m_ξ and m_η

$$\frac{m_\xi}{m_\eta} = \sqrt{\frac{|\left(\frac{\partial^2 u}{\partial \eta^2}\right)|}{|\left(\frac{\partial^2 u}{\partial \xi^2}\right)|}} \tag{91}$$

For the sequel, it will be simpler to express metric $\mathcal{M}$ in terms of the node density d, number of nodes by area unit, and of the local aspect ratio μ :

$$\mathcal{M} = \frac{1}{d}\,\mathcal{R}_{\mathcal{M}}^{-1}\begin{pmatrix} \mu & 0 \\ 0 & \frac{1}{\mu} \end{pmatrix}\mathcal{R}_{\mathcal{M}}\ , \tag{92}$$

More precisely we set: $m_\xi = \sqrt{\frac{\mu}{d}}$ and $m_\eta = \sqrt{\frac{1}{\mu d}}$. Constraint (86) becomes:

$$\int \delta d = 0. \tag{93}$$

Condition (85) can now be written:

$$\begin{gathered}\int \left(|\frac{\partial^2 u}{\partial \xi^2}|\frac{\mu}{d} + |\frac{\partial^2 u}{\partial \eta^2}|\frac{1}{\mu d}\right)^{\alpha-1}. \\ \left(|\frac{\partial^2 u}{\partial \xi^2}|(\frac{\delta\mu}{d} - \frac{\mu\delta d}{d^2}) - |\frac{\partial^2 u}{\partial \eta^2}|\frac{d\delta\mu + \mu\delta d}{\mu^2 d^2}\right) = 0, \\ \forall \delta d \quad \text{such that} \int \delta d = 0\,\text{and}\,\forall\delta\mu.\end{gathered} \tag{94}$$

Let us develop in function of $\delta\mu$ and δd. For $\delta\mu$:

$$\int (*)^{\alpha-1}.\left(|\frac{\partial^2 u}{\partial \xi^2}|\frac{1}{d} - |\frac{\partial^2 u}{\partial \eta^2}|\frac{1}{\mu^2 d}\right)\delta\mu \;=\; 0 \;\; \forall\delta\mu\ , \tag{95}$$

where $(*)$ stands for $|\frac{\partial^2 u}{\partial \xi^2}|\frac{\mu}{d} + |\frac{\partial^2 u}{\partial \eta^2}|\frac{1}{\mu d}$ which, by assumption, never vanishes. We deduce:

$$|\frac{\partial^2 u}{\partial \xi^2}|\frac{1}{d} - |\frac{\partial^2 u}{\partial \eta^2}|\frac{1}{\mu^2 d} = 0. \tag{96}$$

From which we get:

$$\mu = \left(\frac{|\frac{\partial^2 u}{\partial \eta^2}|}{|\frac{\partial^2 u}{\partial \xi^2}|}\right)^{1/2} \tag{97}$$

which is (91). For δd :

$$\int (*)^{\alpha-1} . \left(|\frac{\partial^2 u}{\partial \xi^2}|\frac{-\mu}{d^2} + |\frac{\partial^2 u}{\partial \eta^2}|\frac{-1}{\mu d^2}\right) \delta d \; = \; 0 \; . \tag{98}$$

We get then:

$$(*)^{\alpha-1} \, \frac{1}{d^2} \left(|\frac{\partial^2 u}{\partial \xi^2}|(\mu) + |\frac{\partial^2 u}{\partial \eta^2}|\frac{1}{\mu}\right) = Cte. \tag{99}$$

or, in other words:

$$\frac{1}{d^{\alpha+1}} \; \left(|\frac{\partial^2 u}{\partial \xi^2}|(\mu) + |\frac{\partial^2 u}{\partial \eta^2}|\frac{1}{\mu}\right)^{\alpha} = Cte. \tag{100}$$

Let us replace μ by its value:

$$d^{\alpha+1} = Cte \; \left(|\frac{\partial^2 u}{\partial \xi^2}|.|\frac{\partial^2 u}{\partial \eta^2}|\right)^{\frac{\alpha}{2}} . \tag{101}$$

We thus get:

$$d = C_\alpha \; \left(|\frac{\partial^2 u}{\partial \xi^2}|.|\frac{\partial^2 u}{\partial \eta^2}|\right)^{\frac{\alpha}{2\alpha+2}} . \tag{102}$$

where constant C_α is given by:

$$C_\alpha \;\; = \;\; \left(\int \left(|\frac{\partial^2 u}{\partial \xi^2}|.|\frac{\partial^2 u}{\partial \eta^2}|\right)^{\frac{\alpha}{2\alpha+2}} \;\; dxdy \right)^{-1} \;\; N^2 \; . \tag{103}$$

Finally the square local mesh sizes are given by:

$$m_\xi^2 = C_\alpha^{-1} |\frac{\partial^2 u}{\partial \xi^2}|^{\frac{-2\alpha-1}{2(\alpha+1)}} |\frac{\partial^2 u}{\partial \eta^2}|^{\frac{1}{2(\alpha+1)}} \quad ; \quad m_\eta^2 = C_\alpha^{-1} |\frac{\partial^2 u}{\partial \xi^2}|^{\frac{1}{2(\alpha+1)}} |\frac{\partial^2 u}{\partial \eta^2}|^{\frac{-2\alpha-1}{2(\alpha+1)}} \quad (104)$$

which means that metric $\mathcal{M}_{opt}$ is defined by:

$$\mathcal{M}_{opt} = C_\alpha^{-1} \left(|\frac{\partial^2 u}{\partial \xi^2}|.|\frac{\partial^2 u}{\partial \eta^2}| \right)^{\frac{-\alpha}{2\alpha+2}} \mathcal{R}^{-1} \begin{pmatrix} \left(\frac{|\frac{\partial^2 u}{\partial \eta^2}|}{|\frac{\partial^2 u}{\partial \xi^2}|} \right)^{1/2} & 0 \\ 0 & \left(\frac{|\frac{\partial^2 u}{\partial \xi^2}|}{|\frac{\partial^2 u}{\partial \eta^2}|} \right)^{1/2} \end{pmatrix} \mathcal{R} \ .(105)$$

In the case of the $\mathcal{L}^2$ norm, this becomes:

$$\mathcal{M}_{opt,2} = C_2^{-1} \ \mathcal{R}^{-1} \begin{pmatrix} |\frac{\partial^2 u}{\partial \xi^2}|^{-5/6} |\frac{\partial^2 u}{\partial \eta^2}|^{1/6} & 0 \\ 0 & |\frac{\partial^2 u}{\partial \eta^2}|^{-5/6} |\frac{\partial^2 u}{\partial \xi^2}|^{1/6} \end{pmatrix} \mathcal{R} \ . \qquad (106)$$

The case of the $\mathcal{L}^\infty$ norm can be *formally* derived by passing to the limit:

$$\mathcal{M}_{opt,\infty} = C_\infty^{-1} \ \mathcal{R}^{-1} \begin{pmatrix} |\frac{\partial^2 u}{\partial \xi^2}|^{-1} & 0 \\ 0 & |\frac{\partial^2 u}{\partial \eta^2}|^{-1} \end{pmatrix} \mathcal{R} \ . \qquad (107)$$

And we again get an isorepartition of the integrand of (85).

3.8 Accuracy order

It is possible to extend the error analysis of Section 2.4. In the case of an isotropic adaptation, the value at optimum is:

$$\mathcal{E} = \frac{C}{N} \int_\Omega M^{\frac{\alpha}{\alpha+1}} dxdy \qquad (108)$$

Then second order accuracy will be satisfied if the above integral is bounded. In the case of the 2D Heavyside function equal to unity for positive x, zero else, the largest eigenvalue is necessary the one corresponding to x. Similarly to the 1D case, this second derivative is integrable at best at power one half. For $\alpha = 2$, the power in the optimal error is $2/3$. Thus second order accuracy is not obtained.

In the anisotropic case, the analog computation shows that in order to obtain second order accuracy with the Heaviside function, it is enough that the second $x-$derivative is integrable at power $1/4$, which is true since it is in $L^{1/2}$.

It is then remarkable that the proposed model suggests that isotropic optimal mesh adaption will not produce a second order accurate method in L^2 while the anisotropic optimal mesh adaption will produce such an accuracy. These predictions are in accordance with the results in [7][8].

4 A few numerical experiments

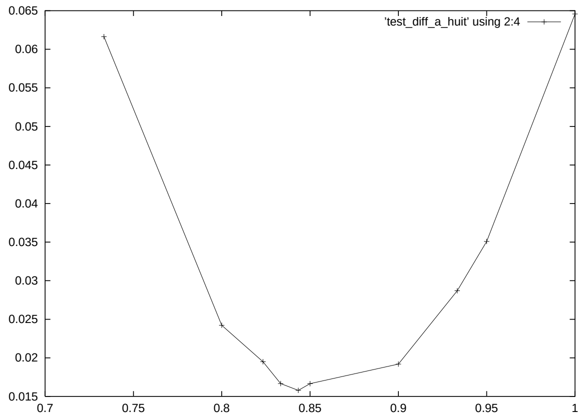

Fig. 1. Optimality of the proposed metric: abscissas are values of the β parameter in the adaptation criterion, ordinates are values of the resulting L^2 interpolation error.

Several issues in our theory desserve numerical illustrations in order to be more convincing.

Firstly, the conclusions of our analysis are valid only if our models are close enough to the discrete context. It is crucial to check that this does not hold only for extremely fine meshes, that could not be used in practice.

Secondly, the ideal meshes that are described as optimal in the case of L^∞ error norm are the ones generally proposed in the literature for solutions of elliptic problems. Now usual error estimates for elliptic problem rely on an Hilbertian theory. We have shown that for the L^2 case, a different family of optimal meshes is found already for the case of an interpolation error. Then it is important to validate our assertion that the second family is somewhat optimal, and to study what qualitative differences appear when we shift from

L^∞ to L^2.

In order to do this, we have to pass to a discrete context. For us, the discrete problem is just a discretization of the continuous optimality system, which expresses the optimal metric as a function of the Hessian of the continuous function to interpolate. The steps for building it consist of :

- building the Hessian, either from analytic differentiation, or, preferably for the sequel, by using a background initial mesh, that is fine enough,

- deriving a metric (continuous or on the background mesh).

From this, we get a discrete solution (the metric on the background mesh) of the continuous problem ("find the metric"). The error of discretization is committed in computing the metric and is related to the quality of the background mesh.

Once the discrete metric is obtained, building the adapted mesh is just a post-treatment. Of course, the main interest is in the adapted mesh and the interpolation on it. We shall focus on the verification of its optimal properties. Before this, we describe how the adapted mesh is built from the metric.

4.1 Mesh adaptation tool

All the presented experiments were achieved thanks to the BAMG software [6]. Given a "background" mesh and an analytic function, BAMG evaluates on the mesh the Hessian of the function by a discrete derivation formula.
We have modified BAMG in order that the metric be computed from the Hessian according to the above formula. Once the metrics is obtained (on nodes of the background mesh), it is used in a mesh regenerator for rebuilding a new mesh following the metrics. The mesh regenerator relies on a Delaunay reconnection in a space mapped by the metric and on vertex addition, again according to the metric. The number of nodes is adjusted when necessary by trial and errors through the modification of the multiplicative coefficient of the metric. Many experiments with BAMG can be found in [14].

4.2 Some optimality

The purpose of this section is to give some numerical experiments showing some optimality of the variational solution proposed.

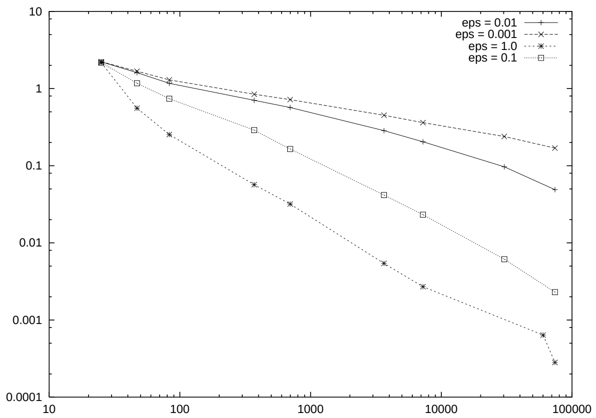

Fig. 2. Convergence to exact function for $\beta = 0.33$, abscissas are numbers of nodes in the meshes used, ordinates are values of the resulting L^2 interpolation error.

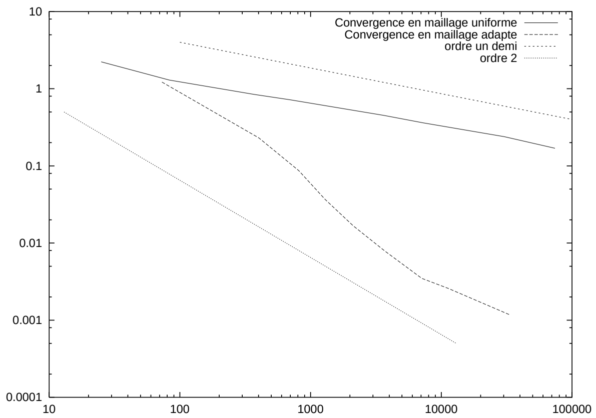

Fig. 3. Convergence to exact function for $\beta = 0.66$, abscissas are numbers of nodes in the meshes used,, ordinates are values of the resulting L^2 interpolation error.

We consider the interpolation on the unit disk of the plane of the following function:

$$f(x,y) \quad = \quad 10x^3 \ + \ y^3 \quad + \quad atan(\frac{\epsilon}{sin(5y) - 2x}) \tag{109}$$

We consider a series of meshes, indexed by a positive β, that all have about 2100 nodes and are adapted according to the following formula:

$$\mathcal{M}_{opt} = \left(|\frac{\partial^2 u}{\partial \xi^2}|.|\frac{\partial^2 u}{\partial \eta^2}| \right)^{\beta} \mathcal{R}^{-1} \begin{pmatrix} \left(\frac{|\frac{\partial^2 u}{\partial \xi^2}|}{|\frac{\partial^2 u}{\partial \eta^2}|} \right)^{1/2} & 0 \\ 0 & \left(\frac{|\frac{\partial^2 u}{\partial \eta^2}|}{|\frac{\partial^2 u}{\partial \xi^2}|} \right)^{1/2} \end{pmatrix} \mathcal{R} \ . \tag{110}$$

This family of metrics involves the usual isorepartition metric, for $\beta = 1$ and the theoretically optimal metric for the L^2 norm, for $\beta = 5/6$ for $\epsilon = .0001$. We then compute the L^2 error. Outputs are depicted in Fig.1. The error norm related to $\beta = 5/6$ is the lowest one, and is about three times smaller the those resulting from $\beta = 0.7$ or from $\beta = 1$.

4.3 Second-order accuracy

In [17] it is claimed that for smooth function with *steep gradients*, uniform mesh refinement show numerical second order convergence only for very fine meshes, and that in contrast best mesh adaptation methods show a property of "early capturing of details", according to which second-order numerical convergence is observed with meshes with a much smaller number of nodes. The purpose of this section is to show examples for which the early capturing of details occurs.

In order to evaluate this phenomenon, we have considered the interpolation of three functions, f_1, f_2, f_3, f_4, of arctangent type 109, with four different "steepness" coefficients: $\epsilon = 1.0, 0.1, 0.01, 0.001$. The mesh convergence is first measured with uniform refinements, Fig.2. When the function is not steep, second order convergence is easily obtained. Conversely, we do not observe it for the steepest one, f_4, even with meshes with almost $100,000$ nodes. We now concentrate on the study on f_4 and adapt the meshes by applying the proposed metric. The effect is a much faster convergence, essentially second order, observable for meshes as coarse as of a few hundred nodes (Fig.3).

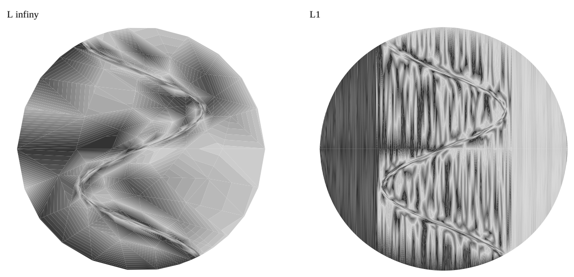

Fig. 4. Representation of a function with the two options, L^∞ (left) and L^2: contours.

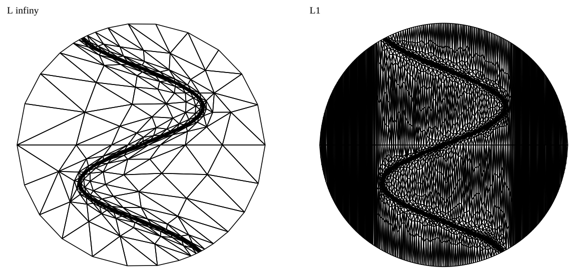

Fig. 5. Representation of a function with the two options, L^∞ (left) and L^2: corresponding meshes.

As mentioned earlier, the proposed variational analysis takes into account the functional space L^α in which we minimize the interpolation error.

The influence of the functional norm will now be studied in relation with the application of a method for image compression.

Indeed, given a function defined on a fine (uniform or not) mesh, a compression could consist of storing it in a smaller mesh, accepting some loss in the accuracy of its definition, as far as the new file is sufficiently small. Mesh adaptive interpolation is an answer to this problem, already used in image processing [15].

The first example will illustrate the better ability of the L_p option with small p to adapt the mesh to the small amplitude details of a function. Let us start with the sum of an arctangent function of amplitude 1., combined this time with a sine function of a ten times lower amplitude.

$$f(x,y) \quad = \quad 0.1 * sin(50x) \quad + \quad atan(\frac{0.001}{sin(5y)-2x}) \tag{111}$$

We compare two adapted meshes with about 2000 nodes each. The first one is adapted following the error isorepartition principle, in other words, by minimizing the L^∞ error functional. The second one is adapted according to the minimization of the L^2 error norm. We observe that L^2 option restitutes the low amplitude sine oscillation while the L^∞ dœs not show it at all.

Mesh-based image compression is particularly useful for storing images produced by numerical finite element computations. As an illustration we consider the compression of the Mach contours of a flow analysis. Conditions of flow calculation is not important for our subject. In Fig.6 we compare the L^∞ and L^2 adapted meshes. The ramp-like shocks starting from the middle of the airfoil correspond to a much smaller amplitude of variation than the vertical bow shock at left part. We observe that they are nearly ignored by the L^∞ option while it is well followed by the L^1 option.

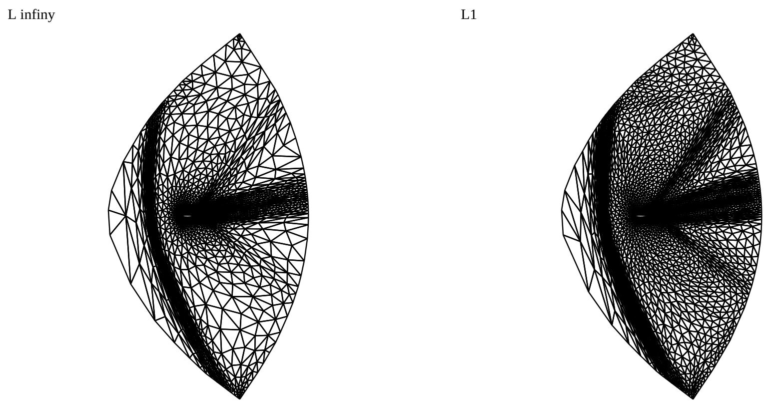

Fig. 6. Mesh-based compression of Mach contours: view of the meshes for L^∞ and L^2 compressions.

A last example is the mesh compression of a black and white portrait of Mona Lisa. The initial image we used is depicted as right-bottom of Fig.7. It was described by a fine adapted mesh of $60,000$ vertices resulting from the image processing presented in [11]. The game is to compress it to only 5000 vertices with the presented algorithm. We have checked that the compression ratio on postscript files is indeed 12.. In that case, the identification of the best approach is not clear. Contrats are important for the vision and some part of the image (the eyes) are more important than other ones. We note however that some regions with low contrast, such as sleeve and hand, Fig.8, are better reproduced with the L^2 option.

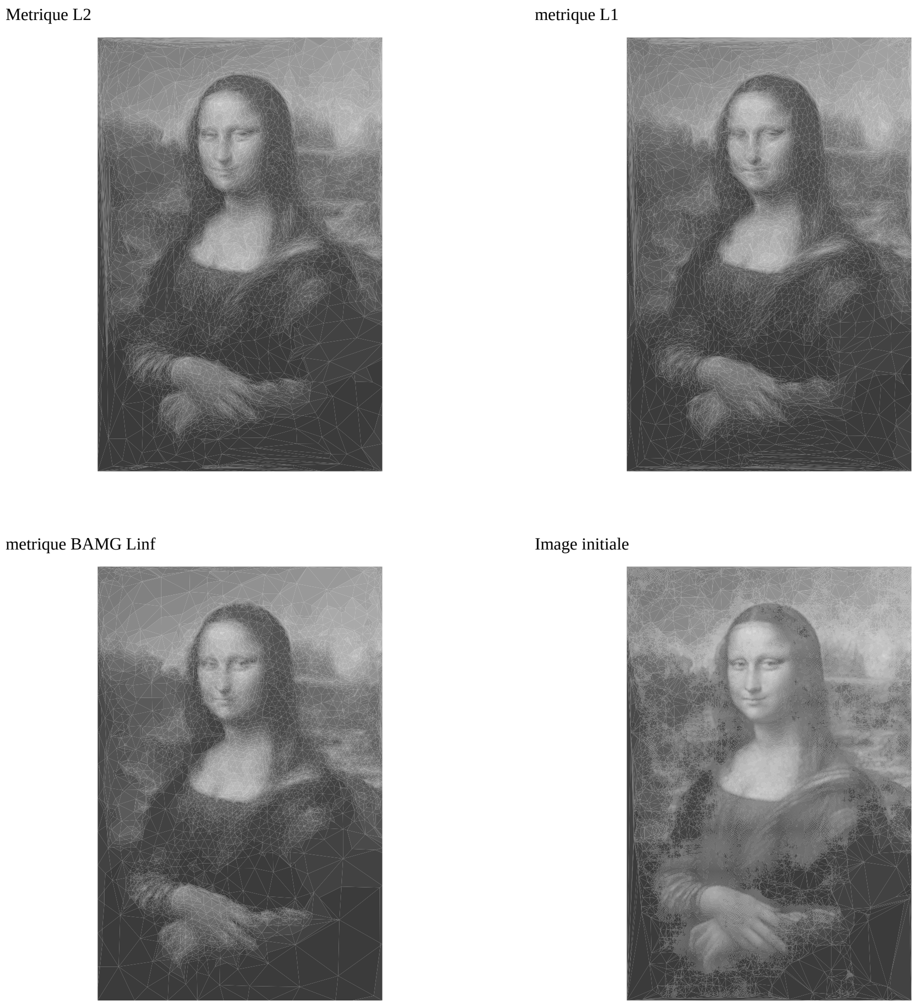

Fig. 7. Mesh-based image compression, global views: initial picture at bottom, L^2 adaptation (top,left), L^1 adaptation (top,right), L^∞ adaptation (bottom,left).

5 Conclusions

This work explores some capabilities of a continuous theory for mesh adaptation.
In this first study, we have restricted us to the problem of best adaptive mesh for pure interpolation.

Mesh is modelled by a metric, the number total of nodes is a continuous integral of the metric, error is modelled with the first term of a Taylor series for the interpolation error.

Once these models are fixed, together with the error norm we want to be the

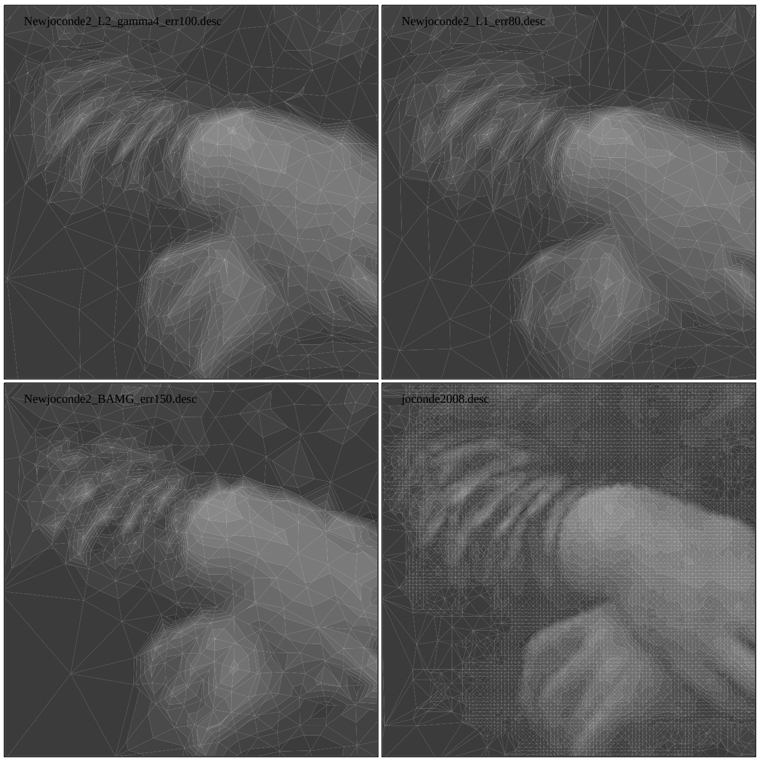

Fig. 8. Mesh-based image compression, zoom: initial picture at bottom, L^2 adaptation (top,left), L^1 adaptation (top,right), L^∞ adaptation (bottom,left).

smallest, the continuous approach provides, by an optimization argument, an answer to the problem of the best possible mesh.

We get a completely explicit expression of the optimal metric in terms of the function to which it is adapted.

This method is also a model for the evaluation of the accuracy order of a mesh adaptive method and can help in specifying conditions for second order accuracy.

Transposition to the discrete context is demonstrated by a few numerical experiments giving some (yet partial of course) confirmation that the approach is sound, efficient and shows the behaviors predicted by the theory.

This type of analysis has a potential usefulness for several applications:

- *in image compression*: the continuous metric method defines an optimal compression method on an isotropic mesh.

- *in scientific computing*. In a future work we follow the strategy proposed here for extending the present method to the research of an optimal mesh for the solution of a PDE.

6 Acknowledgements

Thanks to Herve Guillard for reading this document, Pascal Frey for providing the data related to Mona Lisa.

References

[1] I. Babuska and W.C. Rheinboldt. A posteriori error estimates for finite element method. *Int. J. Numer. Meth. Eng.*, (12):1597–1615, 1978.

[2] R. Becker, M. Braack, and R. Rannacher. Numerical simulation of laminar flames at low mach number with adaptative finite elements. *Combustion Theory and Modelling*, 3:503–534, 1999.

[3] H. Borouchaki and P.L. George. Maillage de surfaces paramétriques. partie I: Aspects théoriques. Technical Report 2928, INRIA Rocquencourt, 1996.

[4] H. Borouchaki and P.L. George. Maillage de surfaces paramétriques. partie II: Exemples d'applications. Technical Report 2944, INRIA Rocquencourt, 1996.

[5] J. Cabello, R. Lohner, and O.-P. Jacquotte. A variational method for the optimization of directionally stretched elements generated by the advancing front method (afm). In A.S. Arcilla, J. Hauser, P.R. Eiseman, and J.F. Thompson, editors, *Numerical Grid Generation in Computational Field Simulation and Related Fields, Proceedings of the 3rd International Grid Conference*, page 521. North Holland, 1991.

[6] M.J. Castro-Diaz, F. Hecht, B. Mohammadi, and P.-L. George. *Anisotropic adaptative mesh generation in two dimensions for CFD*, chapter pp 181-192. Computationals Fluids Dynamic '96, 1996.

[7] Y. Coudiere, B. Palmerio, A. Dervieux, and D. Leservoisier. Accuracy barriers in mesh adaptation. Technical Report 4528, INRIA Sophia-Antipolis, 2002.

[8] A. Dervieux, D. Leservoisier, P.-L. George, and Y. Coudière. About theoretical and practical impact of mesh adaptions on approximation of functions and of solution of pde. In *Conférence invitée ECCOMAS-Swansea.* to appear in I.J.M.N.F., 2001.

[9] L. Formaggia and S. Perotto. Anisotropic error estimates for elliptic problems. *Numer. Math*, 2002.

[10] M. Fortin (Ed.). Estimations a posteriori et adaptation de maillages (partly in french). *Special issue of the Revue Europeenne des Elements Finis*, 2000.

[11] P. Frey. Génération de maillages 3d dans des ensembles discrets. application biomédicale aux méthodes d'éléments finis. Master's thesis, University of Strasbourg I, 1993.

[12] P-J Frey and P-L. George. *Mesh generation.* Hermes, 2000.

[13] W.G. Habashi, J. Dompierre, Y. Bourgault, D. Ait-Ali-Yahia, M. Fortin, and M.-G. Vallet. Anisotropic mesh adaptation: Towards user-independent, mesh-independent and solver-independent cfd solutions: Part I: General principles. *International Journal for Numerical Methods in Fluids*, 32:725–744, 2000.

[14] D. Leservoisier. *Strategies d'adaptation et de raffinement de maillages en Mecanique des fluides.* PhD thesis, Université Pierre et Marie Curie, 2001.

[15] G. Marquant, S Pateux, and C. Labit. Mesh-based scalable image coding with rate-distortion. In *European Signal Processing Conference EUSIPCO 2000*, 2000.

[16] B. Palmerio. Coupling mesh and flow in viscous fluid calculations on unstructured triangular finite element. *Computational Fluid Dynamics*, 6:275–290, 1996.

[17] B. Palmerio and A. Dervieux. Multimesh and multiresolution analysis for mesh adaptive interpolation. *Applied Numerical Mathematics*, 22:477–493, 1996.

[18] B. Tie and D. Aubry. Adaptative FE strategy for non-linear and coupled structural computation. In *Numerical Methods in Engineering '96, Proceeding of the Second ECCOMAS Conference on Numerical Methods in Engineering, 9-13 September 1996*, pages 516–522. John Wiley, 1999.